**Title**
STUDIES OF PARTON FRAGMENTATION AND BARYON PRODUCTION WITH THE TPC AT PEP

**Author**
Madaras, R.J.

**Publication Date**
1986-03-01

LBL-21537 c.2

Lawrence Berkeley Laboratory
UNIVERSITY OF CALIFORNIA

Physics Division

Presented at the XXI Rencontre de Moriond,
Les Arcs, France, March 16-22, 1986

# STUDIES OF PARTON FRAGMENTATION AND BARYON PRODUCTION WITH THE TPC AT PEP

R.J. Madaras

March 1986

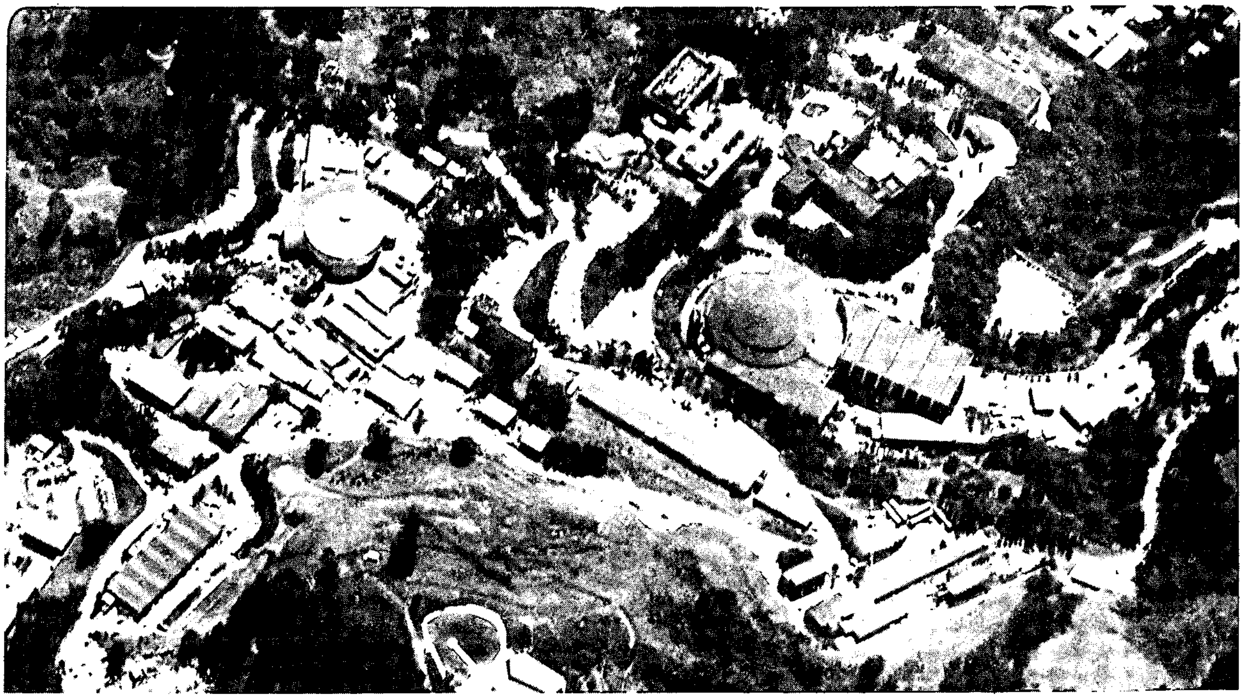

Prepared for the U.S. Department of Energy under Contract DE-AC03-76SF00098

LBL-21537

# STUDIES OF PARTON FRAGMENTATION AND BARYON PRODUCTION WITH THE TPC AT PEP

Ronald J. Madaras
Lawrence Berkeley Laboratory
University of California
Berkeley, CA 94720

Representing the TPC/Two-Gamma Collaboration*

Presented at the
XXI Rencontre de Moriond
Les Arcs, France, March 16-22, 1986

## ABSTRACT

We present here results from the TPC on the analysis of 3-jet events, on the width of gluon jets versus quark jets, and on proton and lambda production and correlations.

*Members of the TPC/Two-Gamma Collaboration are:

H. Aihara, M. Alston-Garnjost, R.E. Avery, A. Barbaro-Galtieri, A.R. Barker, A.V. Barnes, B.A. Barnett, D.A. Bauer, H.-U. Bengtsson, D.L. Bintinger, B.J. Blumenfeld, G.J. Bobbink, A.D. Bross, C.D. Buchanan, A. Buijs, M.P. Cain, D.O. Caldwell, O. Chamberlain, C-Y. Chien, A.R. Clark, G.D. Cowan, D.A. Crane, O.I. Dahl, K.A. Derby, J.J. Eastman, P.H. Eberhard, A.M. Eisner, R. Enomoto, F.C. Erne, T. Fujii, B. Gabioud, J.W. Gary, W. Gorn, J.M. Hauptman, W. Hofmann, J.E. Huth, J. Hylen, U.P. Joshi, T. Kamae, H.S. Kaye, K.H. Kees, R.W. Kenney, L.T. Kerth, Winston Ko, R.I. Koda, R.R. Kofler, K.K. Kwong, R.L. Lander, W.G.J. Langeveld, J.G. Layter, F.L. Linde, C.S. Lindsey, S.C. Loken, A. Lu, X-Q. Lu, G.R. Lynch, R.J. Madaras, K. Maeshima, B.D. Magnuson, J.N. Marx, K. Maruyama, G.E. Masek, L.G. Mathis, J.A.J. Matthews, S.J. Maxfield, S.O. Melnikoff, E.S. Miller, W. Moses, R.R. McNeil, P. Nemethy, D.R. Nygren, P.J. Oddone, H.P. Paar, D.A. Park, D.E. Pellett, M. Pripstein, M.T. Ronan, R.R. Ross, F.R. Rouse, R.R. Sauerwein, K.A. Schwitkis, J.C. Sens, G. Shapiro, M.D. Shapiro, B.C. Shen, W.E. Slater, J.R. Smith, J.S. Steinman, M.L. Stevenson, D.H. Stork, M.G. Strauss, M.K. Sullivan, T. Takahashi, J.R. Thompson, N. Toge, R. van Tyen, B. van Uitert, G.J. VanDalen, R.F. van Daalen Wetters, W. Vernon, W. Wagner, E.M. Wang, Y.X. Wang, M.R. Wayne, W.A. Wenzel, J.T. White, M.C.S. Williams, Z.R. Wolf, H. Yamamoto, M. Yamauchi, S.J. Yellin, C. Zeitlin, W-M. Zhang

Lawrence Berkeley Laboratory, Berkeley, CA; University of California, Davis, CA; University of California Institute for Research at Particle Accelerators, Stanford, CA; University of California, Los Angeles, CA; University of California, Riverside, CA; University of California, San Diego, CA; University of California, Santa Barbara, CA; Carnegie-Mellon University, Pittsburgh, PA; Ames Laboratory, Iowa State University, Ames, IA; Johns Hopkins University, Baltimore, MD; University of Massachusetts, Amherst, MA; New York University, New York, NY; National Institute for Nuclear and High Energy Physics, Amsterdam, The Netherlands; University of Tokyo, Tokyo, Japan

## 1. INTRODUCTION

We report here the analysis of data taken with the Time Projection Chamber[1] (TPC), which provides three-dimensional tracking and dE/dx particle identification, at the PEP electron-positron colliding beam ring. The center-of-mass energy was 29 GeV. The total number of multi-hadronic events in the data is about 29,000 from the 1982-83 run, and about 14,000 from the 1984-85 run. During this latter run the TPC had improved momentum resolution due to the use of a 13.25 kG superconducting coil, and the reduction of drift field distortions with a gated grid[2].

The topics covered in this paper are:

1. Introduction
2. Tests of Parton Fragmentation Models Using 3-jet Events
3. Width of Gluon Jets vs. Quark Jets
4. Baryon Production
5. Conclusions

## 2. TESTS OF PARTON FRAGMENTATION MODELS USING 3-JET EVENTS

The three main types of models for the fragmentation of quarks and gluons into observed hadrons, shown schematically in Figure 1, all have similar predictions for 2-jet events. They differ, however, in their predictions for the distribution of particles between jet axes in 3-jet events.

In the Independent Fragmentation (IF) model[3], each parton fragments independently with cylindrical symmetry in the overall center-of-mass (CM) system. Thus all regions between the jets are populated equally.

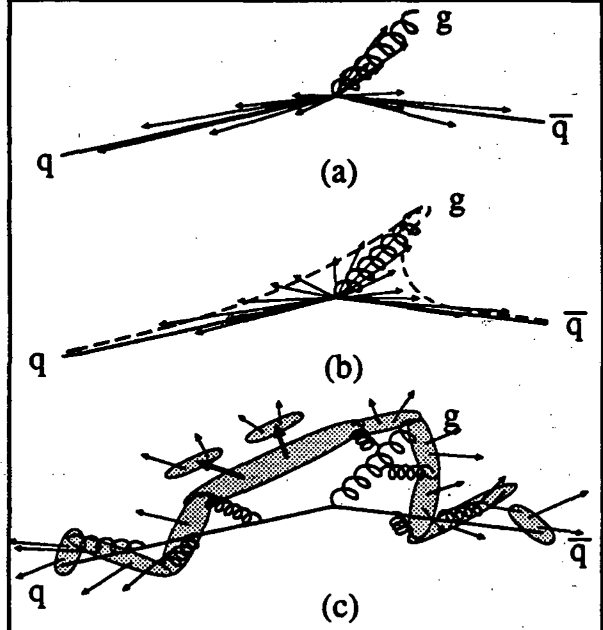

Figure 1 Schematic representation of a 3-jet event in the a) Independent Fragmentation Model
b) String Fragmentation Model
c) Cluster Fragmentation Model

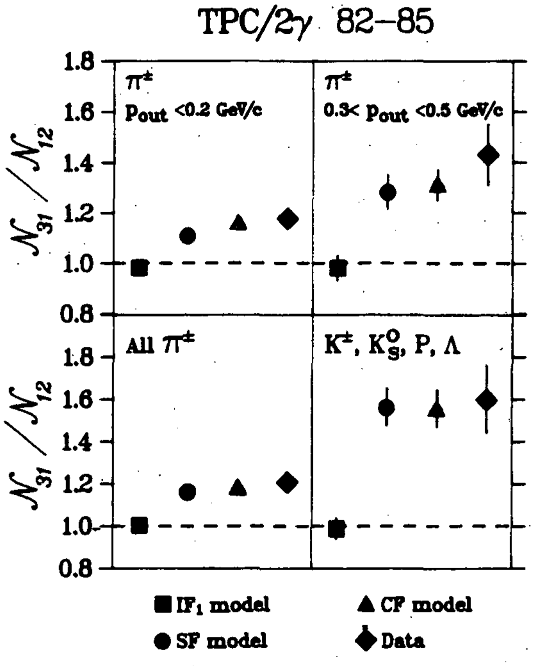

Figure 2 The ratio $N_{31}/N_{12}$ of the population between jets, for the data and models.

In the String Fragmentation (SF) model[4], it is assumed that strings are stretched between the partons along the directions of color flow. Each string fragments in its own rest frame with cylindrical symmetry. The hadrons are boosted to the CM system, thus depleting the region between the q and $\bar{q}$ of hadrons (relative to the gq and $\bar{q}$g regions). Due to its boost origin, this relative depletion effect is enhanced by selecting heavy particles or those particles with a large momentum component out of the event plane ($P_{out}$).

In the Cluster Fragmentation (CF) model[5], the primary partons initiate a quark-gluon shower described by leading-log QCD. After the parton shower evolution, color singlet clusters are formed from neighboring partons, which then decay into hadrons. Soft gluon interference produces an effective angular ordering of gluons, which forces partons in the forward direction along the jet axis. In 3-jet events, this interference effect gives less partons in the $q\bar{q}$ region than in the gq and $\bar{q}$g regions[6].

The 3-jet event selection is described in Reference 7. The jets are labeled 1, 2 and 3 such that jet 1 is opposite the smallest angle between jets and jet 3 is opposite the largest angle. Monte Carlo studies indicate that jet 3 is the gluon jet in about 55% of the events. To search for a depletion of particles in the $q\bar{q}$ region (i.e. between jets 1 and 2), relative to the gq region (i.e. between jets 3 and 1), one calculates $N_{31}/N_{12}$, where $N_{ij}$ is the number of hadrons between jets i and j. For IF models we expect $N_{31}/N_{12} = 1$ independent of the particle mass or $P_{out}$, while for the SF and CF models we expect this ratio to be greater than 1 and to increase in magnitude as mass and $P_{out}$ increase. Figure 2 shows $N_{31}/N_{12}$ for the data and models. It is seen that the IF model fails to describe the data, while the SF and CF models do agree with the data. The failure of the IF model is fundamental, and cannot be explained by parameter tuning or by using different variants of the model.

## 3. WIDTH OF GLUON JETS vs. QUARK JETS

In the SF model (fig. 1b), the gluon has two strings stretched between it and the initial quarks. Each string fragments into hadrons, and thus one would expect that the average transverse momentum (in the event plane) of the hadrons in the gluon jet would be greater than in the quark jets. We have used our 3-jet sample to look for this effect, and find that the ratio of the average transverse momentum (in the event plane) of jet 3 (usually the gluon jet) to jet 2 (the $\bar{q}$ jet) is 1.08 ± 0.02 (preliminary). The SF model predicts 1.10 - 1.11 for this ratio, in agreement with the data. As expected, the IF model gives 0.99 - 1.01 for this ratio, indicating that the effect is not just kinematical. Thus the gluon jet appears to be "fatter" than the quark jets.

## 4. BARYON PRODUCTION

We can use baryon angular distributions and transverse momentum correlations to help distinguish between the baryon production models shown in Figure 3.

In the "fundamental diquark" model[8], it is assumed that diquarks are fundamental entities, and thus diquark-antidiquark pairs can occasionally be formed in the color field (instead of $q\bar{q}$ pairs, which lead to meson production). The combination of a diquark and a quark forms a baryon (fig. 3a).

In the "effective diquark" model[9], it is assumed that occasionally $q\bar{q}$ pairs of non-screening color will "pop" out of the color field. In order to screen the remaining field, another $q\bar{q}$ pair is produced (fig. 3b). These quarks form loosely bound diquarks, which then combine with another quark to form a baryon. In this model, however, it is possible for more than one $q\bar{q}$ pair to be created in the remaining color field, leading to the production of a meson "in between" the baryon and antibaryon (fig. 3c).

In the "cluster decay" model[10], parton showers create low-mass color singlet clusters, some of which may be heavy enough to decay into a baryon and antibaryon (fig. 3d).

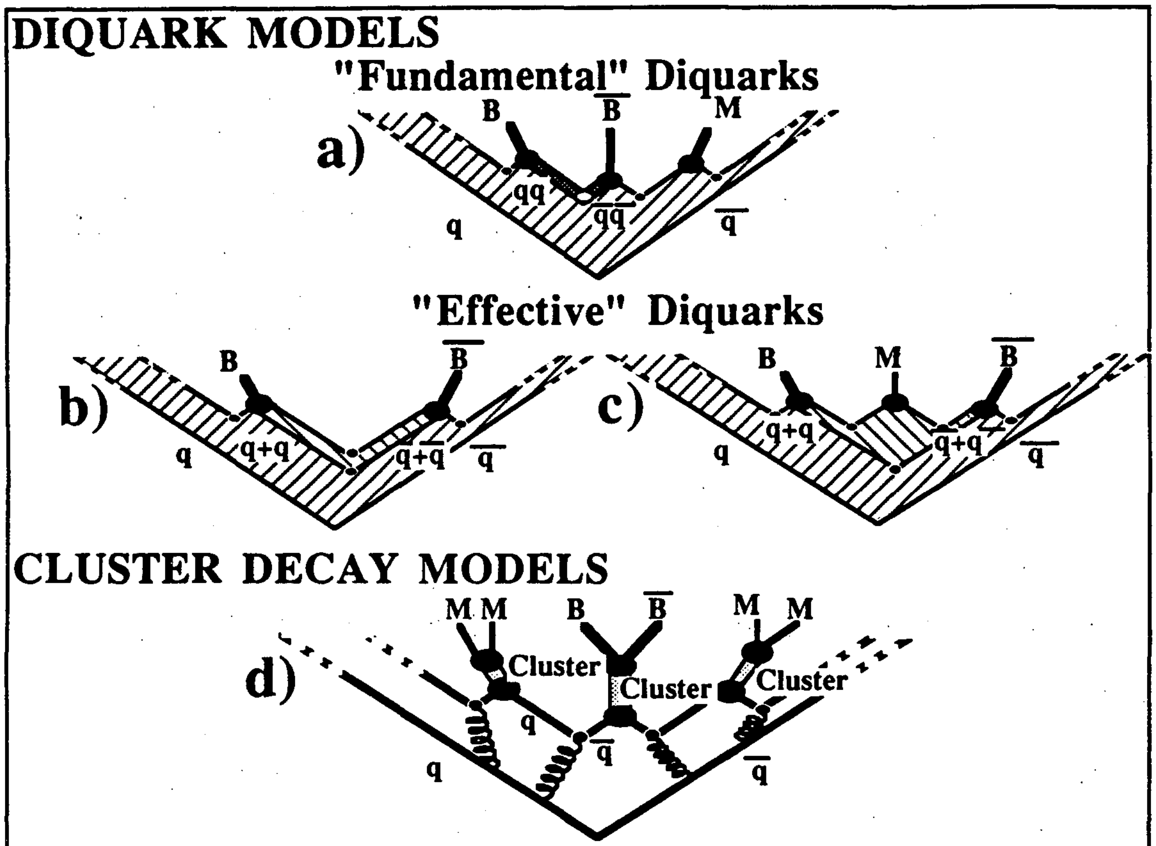

Figure 3 Baryon Production Models

The diquark and cluster models both reproduce the measured inclusive proton spectra quite well[11], but the model predictions differ for the angular dependence of proton-antiproton correlations. If we define the angle $\theta^*$ as the angle between the proton momentum and the jet axis in the CM frame of the $p\bar{p}$ pair, then in the cluster model, since the cluster decays spherically symmetric, the distribution in cos $\theta^*$ will be flat. In both diquark models, the proton and antiproton are more likely to be produced along the jet direction because the diquarks and antidiquarks are pulled apart by the tension in the color string. In this case the angular distributions would show an enhancement at cos $\theta^* = \pm 1$ (fig. 4a).

The cos $\theta^*$ distribution of $p\bar{p}$ pairs measured by the TPC is shown in Figure 4b, together with the predictions of the diquark model and cluster decay model. Because of the limited range of the proton momentum (0.5 - 1.5 GeV/c), the predictions are lower at large cos $\theta^*$ than expected, but the qualitative difference between the two models is maintained. The diquark models (solid curve) are consistent with the data, while the cluster model (dashed curve) disagrees with the data and is excluded at greater than 95% CL. Thus baryon pairs are oriented primarily along the jet axis, and are not produced isotropically in the CM frame of the pair.

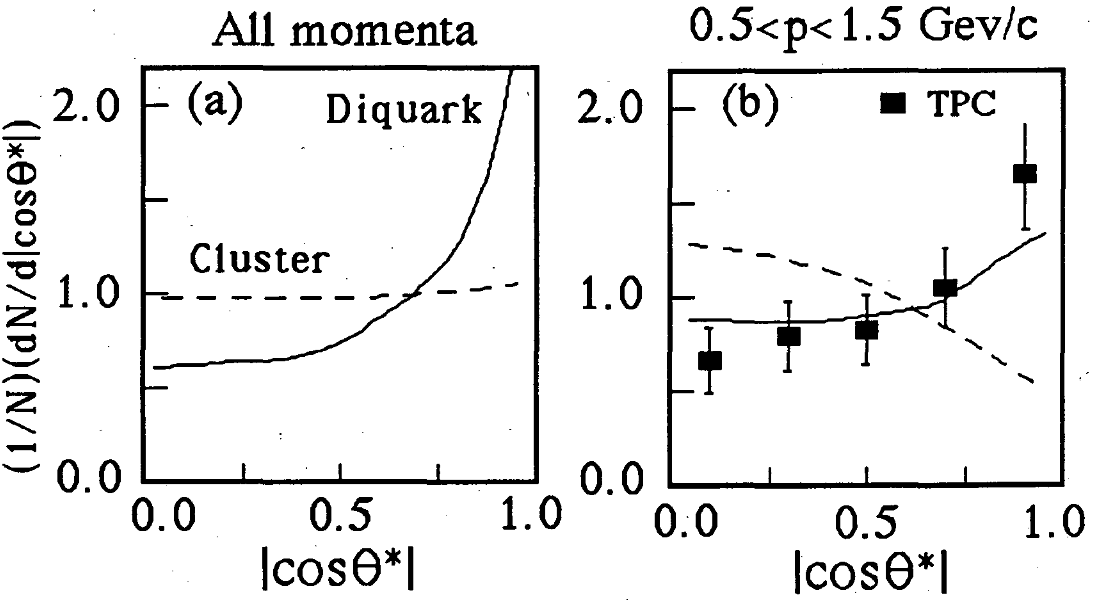

Figure 4 Distribution of $p\bar{p}$ pairs in the angle $\Theta^*$ between the proton direction and the sphericity axis, measured in the $p\bar{p}$ rest frame. a) Predictions of the LUND diquark model (solid line) and of the Webber cluster model (dashed line). b) Experimental points and model predictions, as in a), for momenta between 0.5 and 1.5 Gev/c.

Angular correlations between the p and $\bar{p}$ momentum transverse to the jet axis can discriminate between the two variants of the diquark model[12]. In the "fundamental" diquark model, the diquark and antidiquark will be produced with opposite transverse momenta. In the "effective" diquark model, when a meson is produced between the baryon and antibaryon, this correlation is largely destroyed. We define a correlation coefficient, $\alpha$, proportional to the dot product of the proton and antiproton transverse momentum vectors out of the event plane. Using the "effective" diquark model, one can calculate the value of $\alpha$ as a function of the probability of a $BM\bar{B}$ configuration (i.e. a meson between the baryon and antibaryon). This is shown in Figure 5, along with the value of $\alpha$ measured with the TPC data. It is seen that the probability of a $BM\bar{B}$ configuration is greater than 65% at 90% CL (preliminary). Thus the "effective" diquark model can account for a large part of baryon production.

We can also use baryon correlations to investigate whether baryon number conservation is local or global. First, all multihadron events having an antiproton in the rapidity range of 0.2 - 0.9 are selected. Then for these events we plot the number of protons minus the number of remaining antiprotons as a function of rapidity. The results are in Figure 6, and show an excess of protons at about the same rapidity that was selected for the antiproton, indicating that baryon number conservation is local. The solid curve in Figure 6 is the diquark model prediction, and the dashed curve is just the inclusive rapidity distribution for protons (which one would get if there were no baryon correlations).

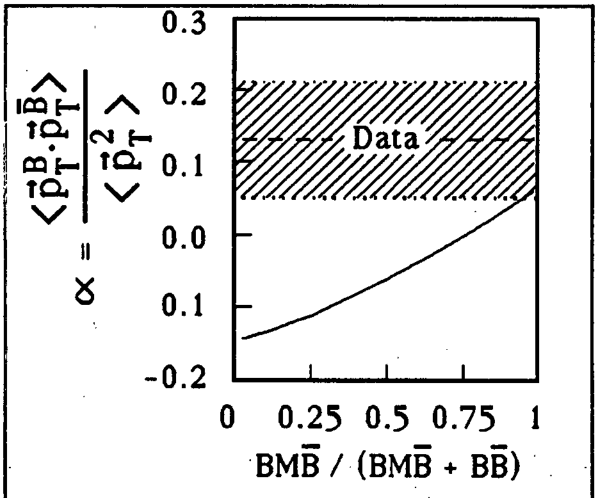

Figure 5 Correlation coefficient $\alpha$ of p,$\bar{p}$ momentum components. Shaded bands: data ±1 SD. Full line: model prediction as a function of the probability to find a $BM\bar{B}$ configuration instead of $B\bar{B}$.

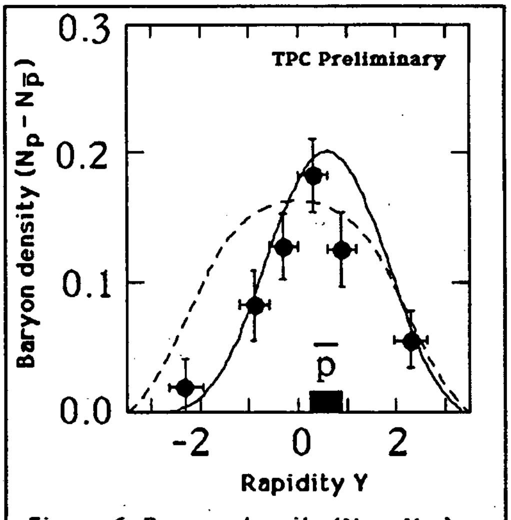

Figure 6 Baryon density $(N_p - N_{\bar{p}})$ after selecting out an antiproton in the rapidity range of 0.2-0.9. Solid curve is the diquark model prediction; dashed curve is the inclusive proton rapidity distribution.

The TPC also sees evidence for local baryon number conservation in events with lambdas and antilambdas, as the $\Lambda\ \bar{\Lambda}$ tend to be in the same jet rather than opposite jets, as the following preliminary results show:

| | Same Jet | Opposite Jet |
|---|---|---|
| $\Lambda\ \bar{\Lambda}$ | 21 events | 6 events |
| $\Lambda\ \Lambda$ | 0 | 2 |
| $\bar{\Lambda}\ \bar{\Lambda}$ | 1 | 1 |

## 5. CONCLUSIONS

The String Fragmentation Model and the Cluster Fragmentation Model satisfactorily predict the relative depletion of hadrons in the region between the q and $\bar{q}$, while the Independent Fragmentation Model fails to describe the data.

We have presented preliminary evidence that gluon jets are "fatter" than quark jets.

We have tested the predictions of various baryon production models using angular correlations between protons and antiprotons, and find that diquark models agree with the data, and cluster models do not. Transverse momentum correlations indicate that the "effective" diquark model can account for a large part of baryon production.

Baryon correlations ($p\bar{p}$ and $\Lambda\ \bar{\Lambda}$) indicate that baryon number is conserved locally.

We acknowledge the efforts of the PEP staff, and the engineers, programmers and technicians of the collaborating Institutions who made this work possible. This work was supported by the United States Department of Energy under contract number DE-AC03-76SF00098, the National Science Foundation, the Joint Japan-United States Collaboration in High Energy Physics, and the Foundation for Fundamental Research on Matter in The Netherlands.

# REFERENCES

1. PEP-4 TPC Collaboration, A. Aihara et al., IEEE Trans. Nucl. Sci. NS30, 63, 76, 162 (1983); N.J. Hadley, Ph.D. thesis, LBL-16116 (1983); R.Z. Fuzesy, N.J. Hadley and P.R. Robrish, Nucl. Instr. and Meth. 223, 40 (1984); J.W. Gary, Ph.D. thesis, LBL-20638 (1985).

2. P. Nemethy et al., Nucl. Instr. and Meth. 212, 273 (1983).

3. P. Hoyer et al., Nucl. Phys. B161, 349 (1979); A. Ali et al., Phys. Lett. 93B, 317 (1983).

4. B. Andersson et al., Phys. Rep. 97, 31 (1983); B. Andersson et al., Z. Phys. C. 20, 317 (1983).

5. B.R. Webber, Nucl. Phys. B238, 492 (1984); T.D. Gottschalk, Nucl. Phys. B214, 201 (1983) and B239, 325, 349 (1984).

6. H. Yamamoto, P. 50; A.H. Mueller, P. 162, Proceedings of the 1985 International Symposium on Lepton and Photon Interactions at High Energies, Kyoto, Japan (1985).

7. PEP-4 TPC Collaboration, H. Aihara et al., Phys. Rev. Lett. 54, 270 (1985) and Z. Phys. C. 28, 31 (1985).

8. B. Andersson, G. Gustafson, and T. Sjostrand, Nucl. Phys. B197, 45 (1982); T. Meyer, Z. Phys. C12, 77 (1982).

9. A. Casher, H. Neuberger, and S. Nussinov, Phys. Rev. D. 20, 179 (1979); B. Andersson, G. Gustafson and T. Sjostrand, University of Lund Report No. LU-TP 84-9, 1984 (unpublished).

10. B.R. Webber, Nucl. Phys. B238, 492 (1984).

11. PEP-4 TPC Collaboration, H. Aihara et al., Phys. Rev. Lett. 55, 1047 (1985).

12. W. Hofmann, Lawrence Berkeley Laboratory Report LBL-20117, Presented at the International Symposium on Multiparticle Dynamics, Kiryat Anavim, Israel (1985).